

Chemical Composition and Corrosiveness of the Condensate in Top-of-the-Line Corrosion

D. Hinkson,^{†*} Z. Zhang,^{**} M. Singer,^{***} and S. Nešić^{***}

ABSTRACT

The three key aspects of the top-of-the-line corrosion process are condensation, chemical speciation, and corrosion. The focus of this study is on the condensate speciation through a thermodynamic approach. Specifically, the goal of this study was to determine the concentration of acetic acid in the condensate. The presence of acetic acid (CH_3COOH) tends to increase the corrosion rate and to promote localized corrosion. The results of this study show that the concentration of free acetic acid in the condensate is determined predominantly by the pH of the liquid phase, which is changed by the corrosion process. The concentration of total acetic acid seems to decrease as the condensation rate increases. The understanding and results gained from this study will lead to the creation of a complete predictive model for top-of-the-line corrosion.

KEY WORDS: acetic acid, condensation, top-of-the-line corrosion

INTRODUCTION

Top-of-the-line corrosion is mutually influenced by three factors. First, the amount of water present on the metal surface at the top of the line is determined by the condensation rate. Second, the composition and distribution of chemical species in the condensate influences the corrosiveness of the condensate. Third, the corrosion process, in turn, influences the conden-

sate chemistry by introducing corrosion products (ferrous ions) and altering the pH and the pH-dependent equilibria. The desire to better describe the mechanistic interaction of these three factors on top-of-the-line corrosion has motivated the present research.

In wet gas pipelines, the main corrosive species are carbon dioxide (CO_2), hydrogen sulfide (H_2S), and organic acids. All of these species can be found in both the gas phase and the liquid phase. From bottom-of-the-line corrosion studies, organic acids are known to increase the risk of corrosion.¹ Since organic acids are volatile, they can be a potential cause of corrosion in the condensed liquid at the top of the line. This begs several questions:

- What is the concentration of organic acids at the top of the line?
- What is the distribution of organic acids between the corrosive, undissociated form and the dissociated form that is not related to metal loss?
- How can the concentration and chemical speciation at the top of the line be predicted?

To answer these questions, acetic acid (CH_3COOH) was chosen as being a representative of the low-molecular-weight organic acids encountered in oil and gas operations, specifically C_1 through C_4 (that is, formic acid (HCOOH), acetic acid, propionic acid ($\text{C}_2\text{H}_5\text{COOH}$) and butanoic acid ($\text{C}_3\text{H}_7\text{COOH}$)). The corrosive and volatile behavior of acetic acid is typical for the low-molecular-weight organic acids. The acid dissociation values of propionic and butanoic acids are similar to that of acetic acid.² The acid dissociation constant of formic acid is ten times larger (or the

Submitted for publication October 13, 2008; in revised form, November 12, 2009.

[†] Corresponding author. E-mail: dezra_hinkson@oxy.com.

* Occidental Petroleum Corporation, 28590 Highway 119, PO Box 1001, Tupman, CA 93276-1001.

** BP America Inc., 501 Westlake Park Blvd., Houston, TX 77079.

*** Institute for Corrosion and Multiphase Technology, Ohio University, 342 West State St., Athens, OH 45701.

pK_a of formic acid is 1 log unit less) than that of acetic acid.³ Despite this, equivalent concentrations of undissociated acetic acid and undissociated formic acid lead to a similar corrosive rate.⁴ Additionally, in most oil and gas fields, acetic acid is the predominant species of organic acid present.

Organic acids can affect the corrosion rate in three ways:

—By increasing the cathodic reaction rate:

Organic acids, for example, acetic acid (here represented as HAc), can increase the cathodic reaction rate by acting as a source of protons (Equation [1]), which then can be reduced (Equation [2]):



—By inhibiting the anodic dissolution reaction:

Crolet, et al., found that acetic acid has a slight inhibiting effect on the anodic dissolution of iron.⁵ Sercombe, et al., also observed inhibition of the corrosion rate by acetic acid at low temperatures (25°C to 40°C), possibly due to a film-forming effect.⁶

—By changing the solubility and protectiveness of the corrosion product films: Crolet and Bonis suggest that acetic acid prevents the precipitation of protective iron carbonate by favoring the soluble iron acetate.² On the contrary, Nafday and Nešić argued that free acetic acid increases the corrosion rate by lowering the pH and not by providing a more soluble corrosion product.⁷ More recently, Fajardo, et al., demonstrated that organic acids increase the amount of time required to form a protective iron carbonate film, thereby lengthening the time during which high corrosion rates can be sustained.⁴

Regardless of the mechanism, it is accepted that the corrosion rate increases as the concentration of acetic acid increases even at the same pH. Specific to the top of the line, Singer, et al., observed that as little as 18 mg/L of free acetic acid is sufficient to almost double the corrosion rate at the top of the line in short-term tests.⁸

Because of the ability of organic acids to increase the corrosion rate, the composition and distribution of organic acids in the condensate at the top of the line was investigated experimentally. A thermodynamic

modeling approach was developed to predict the concentration of acetic acid at the top of the line.

EXPERIMENTAL PROCEDURES

The interaction between condensation, chemical speciation, and corrosion was studied in two series of experiments. In the first series, experiments were performed in non-corroding systems to characterize the influences of condensation and chemical speciation on the resulting condensate chemistry. The second series of experiments went a step further by including the corrosion aspect.

Series 1: Non-Corroding Systems

The non-corroding system studied was $\text{CO}_2/\text{HAc}/\text{H}_2\text{O}$. The objective here was to understand the vapor/liquid partitioning of these species at different condensing conditions, that is, for different condensation rates.

The condensation process supplies the undissociated acetic acid to the condensate according to the vapor/liquid equilibrium.



The condensation of acidic species (organic acids plus dissolved CO_2) leads to a pH decrease.

Series 1: Non-Corroding Systems, Experimental — The experimental setup for this series of tests consisted of a modified distillation apparatus (Figure 1). Two flasks were filled with solutions containing the same concentration of acetic acid. The first flask served as a “prebubbler.” This prebubbler was used to saturate the gas phase with acetic acid and thereby prevent stripping of acetic acid from the second flask, labeled as the “tank.” The “tank” simulated the source of acetic acid to the gas phase, which in a pipeline scenario would be the bottom of the line. The carrier gas, CO_2 , was bubbled through the “prebubbler,” then the “tank,” and finally was allowed to cool and partly condense in the condenser before being vented. Either CO_2 or water was used as the coolant in the condenser, depending on the desired temperature drop that needed to be achieved. After the condensate temperature had stabilized, the condensed liquid was collected by overfilling a sample vial to eliminate the vapor phase, tightly sealing it and storing it under refrigerated conditions until analysis. The concentration of total organic acid was analyzed by ion chromatography using an ion-exclusion column.⁽¹⁾ Typically, 30 min to 1 h were needed to collect a sufficient amount of sample for analysis using this setup. The test parameters are given in Table 1. The temperatures (liquid, vapor, and condensate), gas flow rates (carrier gas and cooling gas), and the concentration of acetic acid (tank liquid and condensate) were all measured and recorded.

⁽¹⁾ By analyzing standard solutions of acetic acid, the systematic error of the ion chromatography method was found to be +10%. Random errors were addressed by performing each analysis on duplicate samples. The average of the duplicated readings were used for the reported acetic acid concentrations.

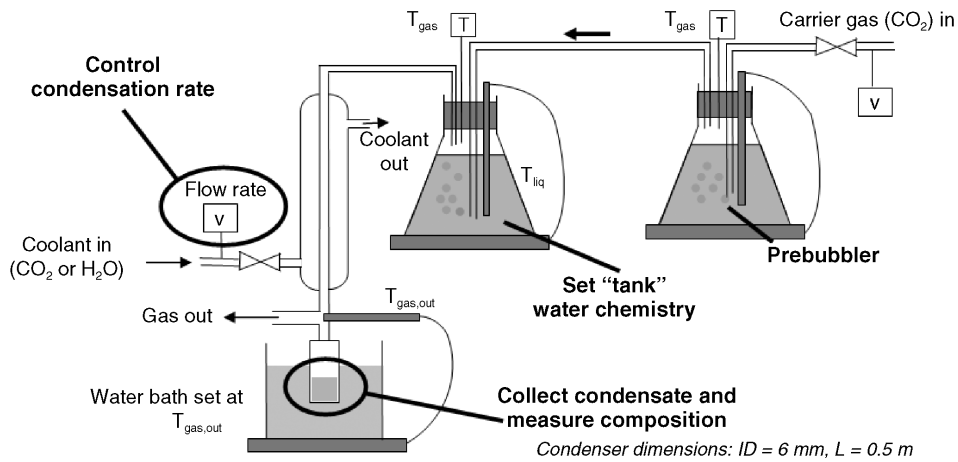


FIGURE 1. Depiction of setup used for Series 1: non-corroding system experiments.

TABLE 1

Test Parameters for Series 1: Non-Corroding Experiments

Parameter	Value(s)
Temperature, $T_{\text{gas,in}}$	68°C ($T_{\text{tank,liq}}$ set at 70°C)
Temperature difference ↔ condensation rate	5, 10, 20, 30, 40°C
Pressure	1 atm
$[\text{HAc, total}]_{\text{tank}}$	1,000 mg/L

Series 1: Non-Corroding Systems, Results — The variation of concentration of total acetic acid in the condensate vs. the temperature drop over which condensation occurred is shown in Figure 2. It was observed that the concentration of total acetic acid in the condensate decreased as the temperature drop for condensation increased, that is, as the condensation rate increased. Since these results are for freshly condensing liquid in the absence of corrosion, the condensate pH was low (~3.5) and there was minimal dissociation of acetic acid to acetate.

Series 2: Corroding Systems

The chemical composition of the condensate is also influenced by the corrosion process (Figure 3). The corrosion process tends to lead to an increase of pH as H^+ ions are consumed by the cathodic reaction (Equation [2]).

In a related study, the change in concentration of free acetic acid in the condensate was found to be influenced predominantly by the liquid equilibrium.⁹ The liquid equilibrium refers to the acid dissociation equilibria in the liquid. The liquid equilibrium is achieved 8 to 10 orders of magnitude faster than the vapor/liquid equilibrium.

Series 2: Corroding Systems, Experimental — The experimental setup shown in Figure 1 was modified for testing the distribution of organic acids in a corroding system (Figure 4). A carbon steel tube was inserted into the condenser such that condensation

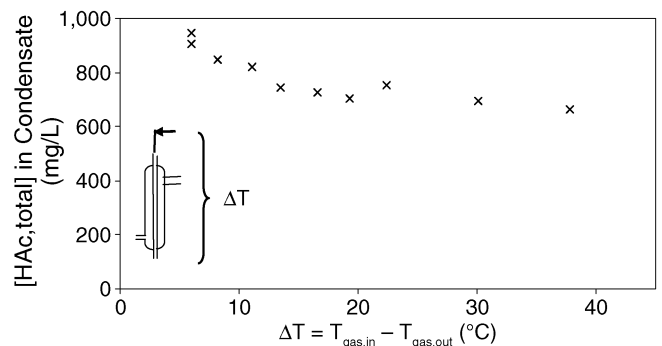


FIGURE 2. Decrease in concentration of total acetic acid with increasing temperature drop for condensation for the non-corroding system.

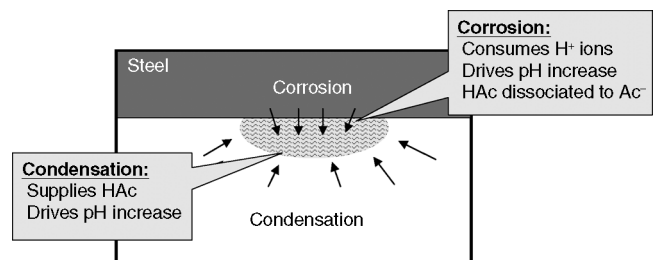


FIGURE 3. Schematic of the key processes influencing the chemical speciation in a droplet.

occurred directly on the inside surface of the steel tube. Thus, the condensation and corrosion processes were studied together.

As in Series 1, the condensation rate was controlled by adjusting the flow rate of the coolant (here, water) and measuring the temperature drop over which condensation occurred. The test matrix is given in Table 2. The condensate was analyzed for the concentrations of total acetic acid (by ion chromatography), dissolved iron (by spectrophotometry), and hydrogen ions (by pH measurement).

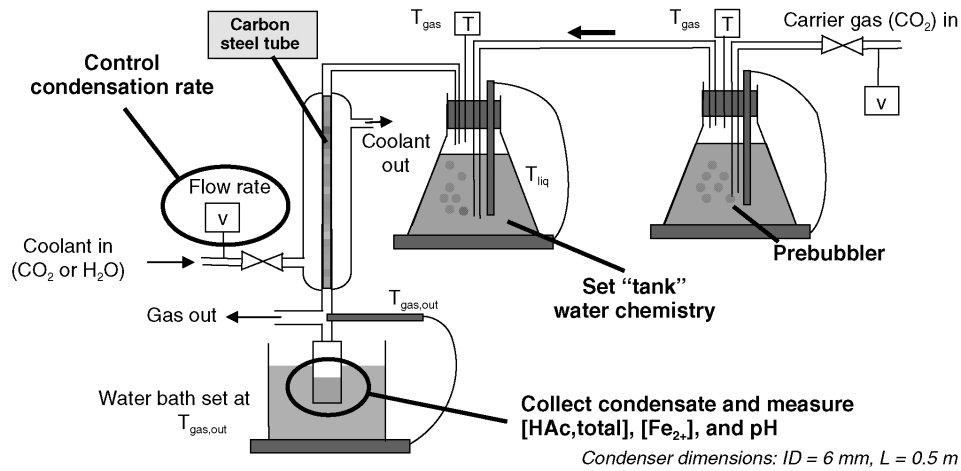


FIGURE 4. Depiction of setup used for Series 2: corroding system experiments.

TABLE 2

Test Parameters for Series 2: Corroding Experiments

Parameter	Value(s)
Temperature, $T_{\text{gas,in}}$	68 °C ($T_{\text{tank,liq}}$ set at 70°C)
Temperature difference ↔ condensation rate	4°C to 16°C
Pressure	1 atm
$[\text{HAc, total}]_{\text{tank}}$	1,200 mg/L

Series 2: Corroding Systems, Results — As with the non-corroding system (Figure 2), it was observed that the concentration of total acetic acid in the corroding system decreased as the temperature drop for condensation increased (Figure 5). The explanation for this behavior is presented in the following section on thermodynamic modeling.

The dissolved iron concentration showed a slightly increasing trend, although there was some scatter in the data (Figure 6). Each of these tests lasted for 2 h but the actual time of contact between the condensing liquid and the corroding steel was much shorter than this. Thus, the vapor/liquid equilibrium was not maintained accurately in these tests.

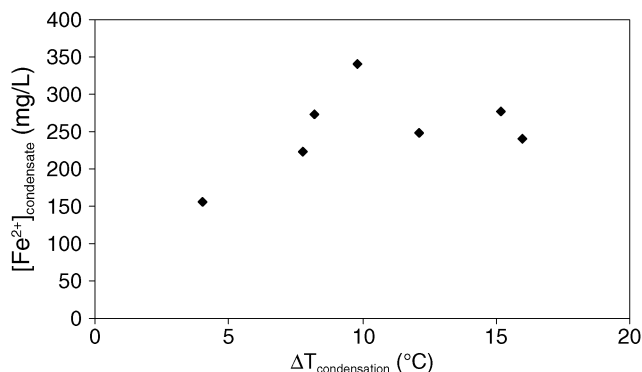


FIGURE 6. Increase of dissolved iron in the condensate as the temperature drop for condensation increased.

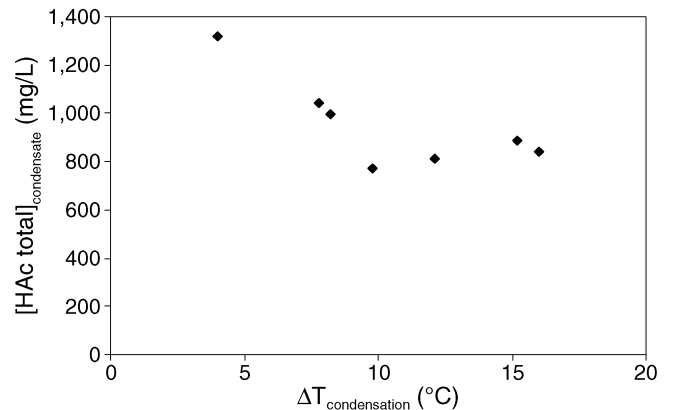


FIGURE 5. Slight decrease in concentration of total acetic acid as the temperature drop for condensation increased.

Consequently, the increase of pH due to the release of ferrous ions by corrosion resulted in dissociation of acetic acid in the condensate. Because the concentration of dissolved iron (and the pH) increased with the temperature drop, the concentration of free acetic acid decreased (Figure 7). It is postulated that in the pipeline scenario, the relatively short droplet res-

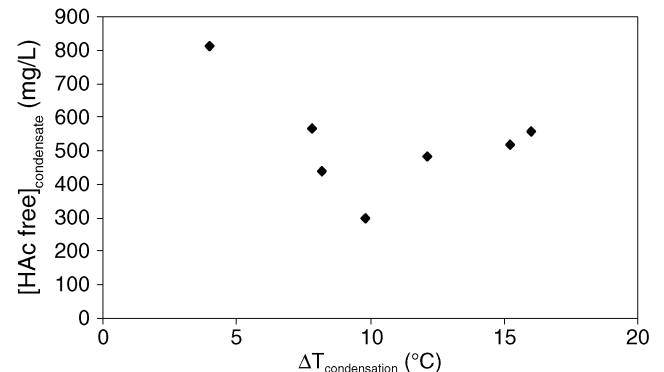


FIGURE 7. Decrease in concentration of free acetic acid in the condensate as the temperature drop for condensation increased.

TABLE 3
Nomenclature

Variable	Unit	Description
$T_{\text{gas,in}}$	Kelvin	Inlet gas temperature of the pipeline section
$T_{\text{gas,out}}$	Kelvin	Outlet gas temperature of the pipeline section
$p_{\text{H}_2\text{O}}(T_{\text{gas}})$	bar	Partial pressure of water at the specified gas temperature, T_{gas} , as calculated by Antoine's equation
V_{liq}	L	Total volume of water that condensed out (assuming condensation rate is given by the dominant species, water only)
$[\text{HAc,free}]_{\text{tank}}$	mol/L	Concentration of undissociated acetic acid in the tank
$[\text{HAc,free}]_{\text{cond}}$	mol/L	Concentration of undissociated acetic acid in the condensate
$H_{\text{HAc}}(T_{\text{gas}})$	mol/L/bar	Henry's law constant for acetic acid calculated at the specified gas temperature, T_{gas}
$H_{\text{CO}_2}(T_{\text{gas}})$	mol/L/bar	Henry's law constant for CO_2 calculated at the specified gas temperature, T_{gas}
$p_{\text{HAc}}(T_{\text{gas}})$	bar	Partial pressure of acetic acid at the specified gas temperature, T_{gas}
$p_{\text{CO}_2}(T_{\text{gas}})$	bar	Partial pressure of CO_2 at the specified gas temperature, T_{gas}
$[\text{CO}_2(\text{l})]$	mol/L	Concentration of dissolved CO_2
$n_{\text{gas,in}}$	moles	Number of moles of acetic acid (or CO_2) present in the gas entering the pipe section, calculated using ideal gas assumption at the inlet gas temperature, $T_{\text{gas,in}}$
$n_{\text{gas,out}}$	moles	Number of moles of acetic acid (or CO_2) present in the gas leaving the pipe section, calculated using ideal gas assumption at the exit gas temperature, $T_{\text{gas,out}}$
$n_{\text{liq,cond}}$	moles	Number of moles of acetic acid (or CO_2) that condenses out into the liquid phase
$K_{\text{HAc,dissoc}}$	mol/L	Dissociation constant of acetic acid; this is only a function of temperature

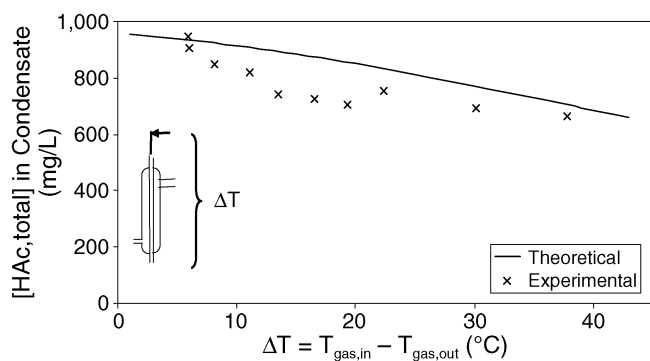


FIGURE 8. Comparison of experimental and theoretical results for Series 1: non-corroding system.

idence time means that a similar situation to this series of tests develops: that the vapor/liquid equilibrium is not sustained and the concentration of free organic acid in the condensate is determined by the pH change due to corrosion.

THERMODYNAMIC MODELING

The system was modeled using a thermodynamic approach wherein steady-state or equilibrium conditions were assumed. First, the modeling of non-corroding systems is presented. The vapor/liquid equilibrium can be described by Henry's law for acetic acid and Antoine's equation for water. In the liquid, the equilibria among aqueous species were described by the acid dissociation expressions. To solve for the concentration of species, the set of equations was completed by applying the conservation of mass (species mass balances) and the conservation of charge (electroneutrality condition). The calculation scheme is given below, and nomenclature is defined in Table 3.

- Define gas temperature: $T_{\text{gas,in}}$ and $T_{\text{gas,out}}$
- $p_{\text{H}_2\text{O}}(T_{\text{gas,in}}) - p_{\text{H}_2\text{O}}(T_{\text{gas,out}}) \rightarrow$ volume condensed, V_{liq}
- Input conditions: $[\text{HAc,free}]_{\text{in}} \rightarrow p_{\text{HAc}}; p_{\text{CO}_2}$

•Henry's Law:
$$p_{\text{HAc}}(T_{\text{gas,out}}) = \frac{[\text{HAc,free}]}{H_{\text{HAc}}(T_{\text{gas,out}})}$$

$$p_{\text{CO}_2}(T_{\text{gas,out}}) = \frac{[\text{CO}_2(\text{l})]}{H_{\text{CO}_2}(T_{\text{gas,out}})}$$

- Mole balance: $n_{\text{gas,in}} = n_{\text{gas,out}} + n_{\text{liq,cond}}$
(Solved for both HAc and CO_2 species.)
- Dissociation in the droplet:

$$[\text{Ac}^-] = \frac{K_{\text{HAc,dissoc}} \cdot [\text{HAc,free}]}{[\text{H}^+]}$$

(Similarly, $\text{CO}_2(\text{l})$ dissociates into H_2CO_3 , HCO_3^- , and CO_3^{2-} .)

The results of the thermodynamic calculations showed that as the temperature drop for condensation increased, the concentration of acetic acid in the condensate decreased. The agreement between these theoretical predictions and the results of the experiments done in a non-corroding system (Series 1) validates the model (Figure 8). Translating the model prediction for a non-corroding system to a pipeline scenario gives the profile for freshly condensing liquid before the onset of corrosion (Figure 9).

In Figure 9 a simulation was done where it was assumed that the concentration at the bottom of the line is constant. Each "droplet" at the top of the line is in equilibrium with the bottom of the line, considering a temperature drop from 70°C to 69°C , 70°C to

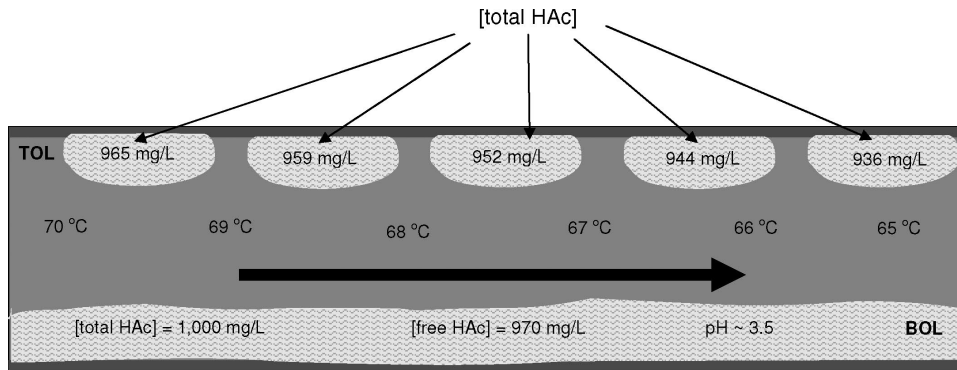


FIGURE 9. Schematic of acetic acid concentration in freshly condensed liquid along a pipeline.

68°C, and so on. Thus, the third “droplet” shows the concentration of total acetic acid expected at the top of the line if the gas was to be condensed from 70°C to 67°C.

Simple reasoning based on the fact that the boiling point of acetic acid is slightly above that of water may lead one to conclude that the concentration of acetic acid should increase as the difference in temperature (or the condensation rate) is increased. However, the observed behavior was contrary to this. This is best explained by considering that the amount of acetic acid in the condensate is related to the change in partial pressure of acetic acid in the gas. As shown in Table 4 and Figure 10, the ratio of the change in partial pressure of acetic acid to the change in partial pressure of water (an indication of the concentration of acetic acid in the condensed liquid) decreased for the larger temperature drop. That is to say, for a larger temperature drop, the condensed liquid is less concentrated in acetic acid due to the relationship between partial pressure and temperature. This data

TABLE 4
Variation of Partial Pressures of Water and Acetic Acid with Temperature Drop

	10°C Temperature Drop (90°C → 80°C)	20°C Temperature Drop (90°C → 70°C)
Δp_{HAc} /bar	6.92×10^{-5}	1.13×10^{-4}
$\Delta p_{\text{H}_2\text{O}}$ /bar	2.33×10^{-1}	3.98×10^{-1}
Ratio of $\Delta p_{\text{HAc}}:\Delta p_{\text{H}_2\text{O}}$	2.98×10^{-4}	2.85×10^{-4}

was calculated using Antoine’s equation for water and Henry’s law for acetic acid, considering a free acetic acid concentration of 1,000 mg/L in the initial liquid phase. It may seem that the ratios of change in partial pressure of acetic acid to that of water were quite small. This is because the data is given in bar/bar and the partial pressure of acetic acid is also quite small. However, it sufficiently illustrates that as the

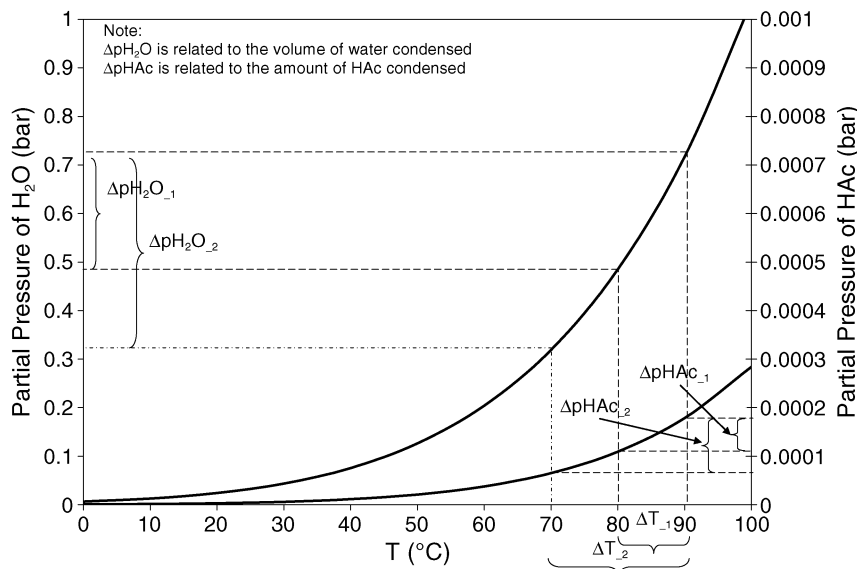


FIGURE 10. Variation of partial pressures of water and acetic acid with temperature.

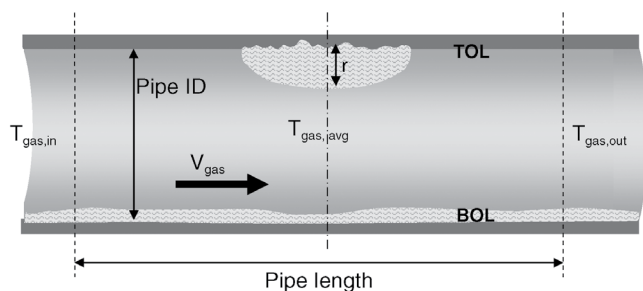


FIGURE 11. Schematic of the model parameters for a pipeline scenario.

temperature drop is increased, the ratio of change in partial pressure of acetic acid to that of water (indicative of the concentration of acetic acid in the condensed liquid) decreases.

This relationship between the change in partial pressure of acetic acid vs. that of water around 70°C is confirmed further by the behavior of the vapor/liquid equilibrium at the boundary conditions. If there is only a minor temperature drop, then the concentration of acetic acid of the condensate at the top of the line more closely compares with the concentration in the source liquid at the bottom of the line. As shown in Figure 9, a bottom-of-the-line free acetic acid concentration of 970 mg/L corresponds with a top-of-the-line acetic acid concentration of 965 mg/L for a temperature drop of 1°C (from 70°C to 69°C). At the other extreme, if the gas is condensed completely, then the concentration of acetic acid in the condensate is comparable with the concentration of acetic acid in the gas phase. A bottom-of-the-line free acetic acid concentration of 970 mg/L is in equilibrium with ~670 mg/L of acetic acid in the vapor phase (at 70°C). If all this vapor was condensed completely, the concentration of acetic acid in the condensate would be equal to the concentration in the gas phase, ~670 mg/L. Between these two extremes, there is a decrease in concentration of acetic acid in the condensate with increasing temperature drop, which is approximately linear (see theoretical results in Figure 8.)

The experimental work and calculations described above have led to two important conclusions, which can be used as the starting point to determine the distribution of chemical species in a corroding system. First, the above experiments prove that the thermodynamic approach can be used successfully to predict the concentration of species in freshly condensed liquid. Second, the distribution of species in the condensate is influenced predominantly by the liquid equilibrium and more specifically, the pH. These findings will be used as the assumptions when considering the corroding system.

For the corroding system, the calculation scheme given earlier in this section was used to obtain the concentration of total organic acid in the condensate. The acid dissociation in the condensate was then

evaluated based on modifying the charge balance to include ferrous ions (Equation [5]).



A concentration of ferrous ions was introduced into the model and the concentration of all species was recalculated to restore equilibrium. The concentration of ferrous iron was then increased incrementally to simulate what would happen as the steel corroded. Reiterations were done until the condensate was supersaturated with iron carbonate. The model developed and tested with a benchtop apparatus was then extended to model the condensate chemistry in a corroding pipeline.

MODELING THE CONDENSATE COMPOSITION IN A PIPELINE

For the pipeline scenario (Figure 11), typically the gas temperature and gas flow rate are known. For this illustration, the condensation rate is specified and the temperature of the gas leaving the pipe section was calculated. Depending on the data available, it is also possible to use the gas temperatures (inlet and outlet) as inputs and to calculate the condensation rate from these.

To calculate the concentration of species in the top-of-the-line condensate, it is necessary to know the pH and concentration of volatile species in the bottom of the line. The thermodynamic modeling approach described in this paper was applied using the baseline conditions shown in Table 5. The model predictions gave the evolution of the concentration of species with time (Figure 12).

Initially, at time = 0 h, the acetic species exist almost completely as undissociated acid. This is because the initial pH is low (~3.3). However, as the time increases, ferrous ions are released into solution by the corroding steel and the pH increases. This results in an increase in the acetate concentration accompanied by a proportionate decrease in free acetic acid concentration. The concentrations of total acetic acid and of dissolved CO₂ are constant because of the assumption that the time needed to achieve and maintain vapor/liquid equilibrium is too slow relative to the droplet residence time. The concentration and distribution of all chemical species are thus defined. The simulation was truncated when the iron carbonate saturation was achieved, which, in this case, occurred after 1.25 h.

CONCLUSIONS

❖ The concentration of total organic acid in the condensate at the top of the line can be predicted by a thermodynamic consideration of the vapor/liquid equilibrium.

TABLE 5
Input Parameters for Model Simulation of the Condensate Chemistry in a Corroding Pipeline

Parameter	Description	Baseline Value
$T_{\text{gas,in}}$	Gas temperature entering the pipe section	70°C
$T_{\text{gas,out}}$	Gas temperature leaving the pipe section	Calculated based on the condensation rate
$T_{\text{gas,avg}}$	Average gas temperature in the pipe section	Calculated based on the condensation rate
P_{total}	Total pressure	3 bar
$p\text{CO}_2$	Partial pressure of CO_2	2 bar
Cond.rate	Condensation rate	0.25 mL/m ² /s
CR_{TOTL}	Corrosion rate at the top of the line	0.25 mm/y
$[\text{HAc total}]_{\text{BOL}}$	Concentration of total acetic acid at the bottom of the line	100 mg/L
pH_{BOL}	pH at the bottom of the line	4
v_{gas}	Gas flow rate	5 m/s
Pipe ID	Pipe internal diameter	10 cm
L	Pipe length	1 m
r	Droplet radius	5 mm
t	Maximum residence time of a droplet	100 min

❖ The distribution of organic acid in the condensate between dissociated and undissociated forms is influenced predominantly by the pH of the condensate as determined by the increase in dissolved ferrous concentration due to corrosion and less influenced by the condensation process and vapor/liquid equilibrium once corrosion is initiated.

❖ As the condensation rate increases, the concentration of organic acid in the condensate decreases. That is, a low condensation rate would present a more concentrated solution of the organic acids at the top of the line than a higher condensation rate would.

❖ This thermodynamic approach can be applied to other species that are known to be problematic from a corrosion point of view, such as CO_2 and H_2S .

❖ The above methodology for the prediction of the concentration of corrosive species in the condensate allows the corrosion rate at the top of the line to be determined accurately from mechanistically sound principles.

ACKNOWLEDGMENTS

The author is grateful for the technical support of the staff at the Institute for Corrosion and Multiphase Technology, Ohio University, and for organic acid analysis provided by J. Thompsen, ConocoPhillips. This work was made possible through the financial support and technical guidance of the following companies: ConocoPhillips, Total, ENI, and BP.

REFERENCES

1. S. Nešić, "Key Issues Related to Modeling of Internal Corrosion of Oil and Gas Pipelines—A Review," 16th Int. Corros. Cong., Key-

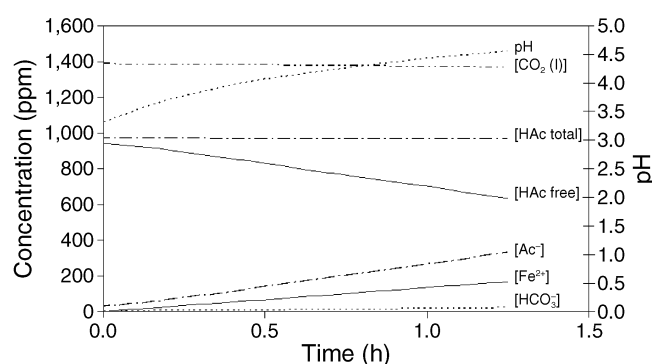


FIGURE 12. Evolution of concentration profiles within a droplet.

note Address (Beijing, China: International Corrosion Council, September 2005).

2. J.L. Crolet, M. Bonis, "Why So Low Free Acetic Acid Thresholds, in Sweet Corrosion at Low P_{CO_2} ," CORROSION/2005, paper no. 272 (Houston, TX: NACE International, 2005).
3. M. Tomson, A. Kan, G. Fu, L. Cong, M. Al-Thubaiti, "A New Theoretically Accurate Method to Measure Alkalinity," CORROSION/2004, paper no. 04074 (Houston, TX: NACE, 2004).
4. V. Fajardo, C. Canto, B. Brown, S. Nešić, "Effect of Organic Acids in CO_2 Corrosion," CORROSION/2007, paper no. 07319 (Houston, TX: NACE, 2007).
5. J.L. Crolet, N. Thevenot, A. Dugstad, "Role of Free Acetic Acid on the CO_2 Corrosion of Steels," CORROSION/1999, paper no. 466 (Houston, TX: NACE, 1999).
6. M. Sercombe, S. Bailey, R. De Marco, B. Kinsella, "An Investigation of the Influence of Acetic Acid on Carbon Dioxide Corrosion," Proc. Corrosion Prevention Conf., paper no. 22 (Perth, Australia: Australian Corrosion Association Inc., 2004).
7. O.A. Nafday, S. Nešić, "Iron Carbonate Film Formation and CO_2 Corrosion in the Presence of Acetic Acid," CORROSION/2005, paper no. 05295 (Houston, TX: NACE, 2005).
8. M. Singer, S. Nešić, Y. Gunaltun, "Top-of-the-Line Corrosion in Presence of Acetic Acid and Carbon Dioxide," CORROSION/2004, paper no. 04377 (Houston, TX: NACE, 2004).
9. D. Hinkson, "A Study of the Chemical Composition and Corrosivity of the Condensate for Top-of-the-Line CO_2 Corrosion" (Master's thesis, Ohio University, 2007).